The Shb scaffold binds the Nck adaptor protein, p120 RasGAP, and Chimaerins and thereby facilitates heterotypic cell segregation by the receptor EphB2

Received for publication, May 14, 2019, and in revised form, February 7, 2020 Published, Papers in Press, February 14, 2020, DOI 10.1074/jbc.RA119.009276

Melany J. Wagner[‡§1], Marilyn S. Hsiung[§], Gerald D. Gish[§], Rick D. Bagshaw[§], Sasha A. Doodnauth[‡], Mohamed A. Soliman[§], Claus Jørgensen[¶], Monika Tucholska[§], and Robert Rottapel[‡‖2]**

*From the [‡]Princess Margaret Cancer Centre, University Health Network, Toronto, Ontario M5S 1A8, Canada, the [§]Lunenfeld-Tanenbaum Research Institute, Mount Sinai Hospital, Toronto, Ontario M5G 1X5, Canada, the [¶]Cancer Research UK Manchester Institute, University of Manchester, Alderley Park SK10 4TG, United Kingdom, the [‖]Departments of Medicine, Immunology and Medical Biophysics, University of Toronto, Toronto, Ontario M5S, Canada, and the **Division of Rheumatology, St. Michael's Hospital, Toronto, Ontario M5B 1W8, Canada*

Edited by Alex Toker

Eph receptors are a family of receptor tyrosine kinases that control directional cell movement during various biological processes, including embryogenesis, neuronal pathfinding, and tumor formation. The biochemical pathways of Eph receptors are context-dependent in part because of the varied composition of a heterotypic, oligomeric, active Eph receptor complex. Downstream of the Eph receptors, little is known about the essential phosphorylation events that define the context and instruct cell movement. Here, we define a pathway that is required for Eph receptor B2 (EphB2)–mediated cell sorting and is conserved among multiple Eph receptors. Utilizing a HEK293 model of EphB2$^+$/ephrinB1$^+$ cell segregation, we found that the scaffold adaptor protein SH2 domain–containing adaptor protein B (Shb) is essential for EphB2 functionality. Further characterization revealed that Shb interacts with known modulators of cytoskeletal rearrangement and cell mobility, including Nck adaptor protein (Nck), p120-Ras GTPase-activating protein (RasGAP), and the α- and β-Chimaerin Rac GAPs. We noted that phosphorylation of Tyr^{297}, Tyr^{246}, and Tyr^{336} of Shb is required for EphB2–ephrinB1 boundary formation, as well as binding of Nck, RasGAP, and the chimaerins, respectively. Similar complexes were formed in the context of EphA4, EphA8, EphB2, and EphB4 receptor activation. These results indicate that phosphotyrosine-mediated signaling through Shb is essential in EphB2-mediated heterotypic cell segregation and suggest a conserved function for Shb downstream of multiple Eph receptors.

Eph receptors are the largest family of receptor tyrosine kinases and play a distinct role in development, homeostasis, and cancer. The family is subdivided into two groups, composed of nine EphA receptors and five EphB receptors that participate in preferential binding to ligands within the ephrinA and ephrinB families, respectively. A well-defined cellular function of the Eph receptor is mediating directional cell movement during tissue boundary formation and axon guidance (reviewed in Ref. 1). For example, EphB2 and EphB3 control homeostatic cell positioning within the intestinal crypts (2), whereas the EphA4 receptor controls axon guidance during formation of the cortical spinal tract (3–7). Because the Eph receptors also appear to play a complex role in tumor formation and growth, they have recently become the focus of clinical investigations for potential therapeutic intervention (reviewed in Ref. 8).

Although these receptors use phosphotyrosine-mediated signals to alter cytoskeletal function, the biochemical mechanisms involved are complex and poorly defined. This is due, in part, to the diverse nature of receptor activation. To initiate signaling, a tetrameric or higher order complex forms consisting of at least two ephrins bound to two Eph receptors (9, 10). A variety of Eph receptors and ephrin family members can participate in any given complex. In fact, the complex can expand to include both EphA and EphB receptors, as well as receptors that are not bound by ephrins (11, 12). The resulting downstream signaling pathways depend on the composition of Eph receptors in the assembly (12). Eph receptors activate diverse biochemical pathways by virtue of their unique intracellular domains that recruit a distinct set of proximal signaling effector proteins.

To deconvolute Eph receptor signaling underlying the process of cell segregation, we undertook an siRNA screen in cell lines that overexpress EphB2 or its ligand ephrinB1 (13). Potential proteins of interest were then evaluated by quantitative MS for signaling-induced changes in phosphotyrosine levels. Because bidirectional signaling downstream of the Eph receptor and the ephrin ligand controls directed cell movement, we utilized isotopic labeling to distinguish phosphotyrosine-mediated signals in Eph receptor and ephrin-expressing cells, respectively. This approach revealed the SH2 domain–containing scaffold protein Shb as an effector of Eph and ephrin signaling pathways.

This work was supported by a foundation grant from the Canadian Institutes for Health Research (to R. R.). The authors declare that they have no conflicts of interest with the contents of this article.
This article contains Figs. S1–S5.

[1] Supported by a fellowship from the Canadian Institutes of Health Research. To whom correspondence may be addressed. Tel.: 647-289-7555; E-mail: mjdwagner@hotmail.com.
[2] To whom correspondence may be addressed: University of Toronto, PMCRT–MaRS, 101 College St., Rm. 12-704, Toronto, ON M5G 1L7, Canada. Tel.: 416-581-7852; Fax: 416-595-5719; E-mail: rottapel@gmail.com.

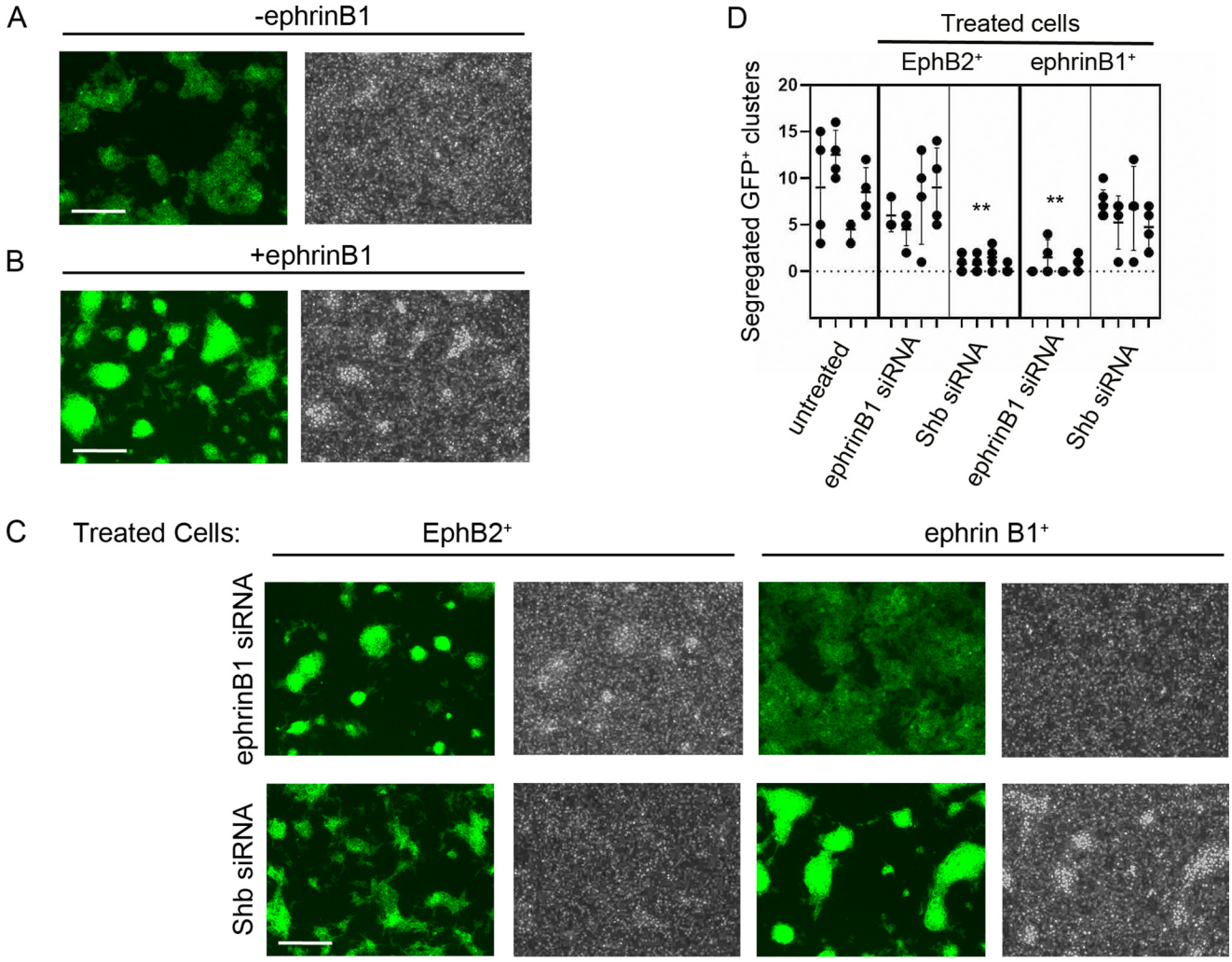

Figure 1. Shb is required downstream of EphB2 in EphB2–ephrinB1 cell sorting. HEK293 cells expressing EphB2 and a myristoylated GFP were co-cultured for 4 days with HEK293 expressing ephrinB1. Fluorescent microscopy detected segregation of the GFP^+ and GFP^- cell lines within a confluent monolayer (*left panel*), and confluency was visualized by Hoescht-stained nuclei (*right panel*) (10× magnification). *A*, negative control: $EphB2^+GFP^+$ HEK293 co-incubated with parental HEK293 (−ephrinB1). *Scale bar*, 300 μm. *B*, positive control: co-incubation of untreated $EphB2^+GFP^+$ HEK293 incubated with $ephrinB1^+$ HEK293 (+ephrinB1). *Scale bar*, 300 μm. *C*, the effects of siRNA against ephrinB1 and Shb were assessed in each cell type. *Scale bar*, 300 μm. *D*, efficient segregation was enumerated by a manual count of compact clusters of GFP^+ cells per field of view. The plot shows the means ± standard deviation for four separate experiments ($n = 3$, $n = 4$, $n = 4$, and $n = 4$). Significant differences for siShb and ephrinB1 treatment compared with untreated cultures are marked. **, $p < 0.005$.

Shb is an SH2 domain–containing scaffold protein with many phosphotyrosine motifs located within a long disordered N terminus (14, 15). Shb is phosphorylated on multiple tyrosine residues following activation of c-Met, epidermal growth factor receptor, or colony-stimulating factor-1 receptor and in response to fibroblast growth factor 2 (16). Shb phosphorylation has also been reported downstream of the T-cell receptor (17), focal adhesion kinase (18), and the viral protein LMP2A (19).

We previously demonstrated that Shb was required for *in vitro* boundary formation between $EphB2^+$ cells and $ephrinB1^+$ cells (13). However, the role of Shb during Eph or ephrin signaling remained unclear. Here we show that phosphorylated Shb binds known modulators of the cytoskeleton and polarized mobility, specifically Nck, p120 RasGAP, and Chimaerins, and these interactions enable EphB2-mediated heterotypic cell segregation.

Results

We previously identified Shb as a potential signaling protein required for Eph- and ephrin-mediated *in vitro* cell sorting in a large-scale siRNA screen in HEK293 cells (13). To determine whether Shb is required in both $EphB2^+$ and $ephrinB1^+$ cells or in only one cell type, we depleted Shb in each cell line and then reconstituted with the untreated heterologous cells in the sorting assay. HEK293 cells expressing a membrane-anchored GFP and EphB2 ($EphB2^+$) were co-incubated with HEK293 cells expressing ephrinB1 ($ephrinB1^+$) or parental HEK293 cells, as a negative control. After a 3-day period, the confluent monolayer was visualized by Hoescht-stained nuclei, and distribution of $EphB2^+$ cells was monitored by the fluorescence of co-expressed GFP (Fig. 1). Compared with the negative control, where $EphB2^+$ cells were co-incubated with parental HEK293 (Fig. 1*A*), incubation with ephrinB1-expressing cells forced the $EphB2^+$ cells into compact clusters with cell crowding toward

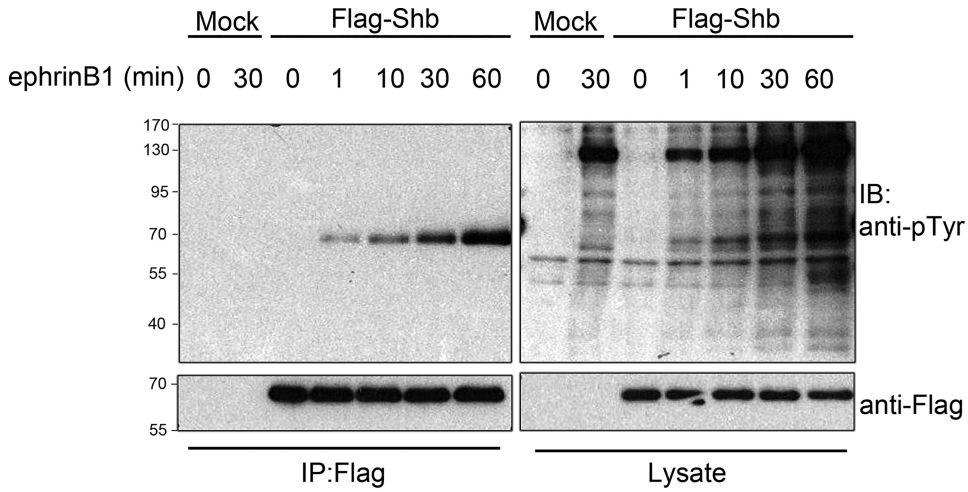

Figure 2. EphB2 signaling enhances tyrosine phosphorylation of Shb. EphB2$^+$ HEK293 were transfected with FLAG-tagged Shb (*FLAG-Shb*) and empty vector (*Mock*). The cells were stimulated with soluble, cross-linked ephrinB1 for 0, 1, 10, 30, and 60 min. Immunoprecipitation (*IP*) of FLAG-tagged Shb and immunoblotting (*IB*) analysis of FLAG and phosphotyrosine were used to identify phosphorylated Shb. Molecular mass (kDa) is indicated to the *left* of the panel.

an elevated center and smooth, rounded borders (Fig. 1*B*). These clusters are evident through visualization of GFP or the tightly packed Hoescht-stained nuclei (Fig. 1*B*). Knockdown of ephrinB1 by siRNA in ephrinB1$^+$ cells, but not EphB2$^+$ cells, impaired heterotypic cell segregation (Fig. 1, *C* and *D*). Similarly, Shb siRNA treatment of the EphB2$^+$ cells and not the ephrinB1$^+$ cells impaired EphB2–ephrinB1 cell sorting. A time-lapse analysis of the Shb-depleted EphB2$^+$GFP$^+$ cell clusters that remained indicated that the clusters formed within 48 h after seeding but failed to develop sharper borders and become more compact at later times (Fig. S1). Thus, Shb primarily interacts with the EphB2 receptor to enhance the formation of boundaries between EphB2- and ephrinB1-expressing cells.

Quantitative MS identified Shb as one of the most highly tyrosine-phosphorylated proteins in the EphB2-expressing cells upon co-incubation with ephrinB1-expressing cells, suggesting a phosphotyrosine-mediated scaffold function for Shb (13). Using soluble, cross-linked ephrinB1 to stimulate EphB2-expressing HEK293, we examined the time course of Shb phosphorylation (Fig. 2). Over the time period monitored, up to 60 min after ligation, a steady increase in Shb phosphorylation was observed, as detected by anti-phosphotyrosine Western blotting analysis. This temporal pattern also correlated with global changes to tyrosine phosphorylation in the whole cell lysate.

To identify proteins associated with Shb during EphB2 signaling, we performed MS on Shb isolates from EphB2$^+$ HEK293 cells stably expressing FLAG epitope-tagged Shb (Shb$^+$EphB2$^+$). Nonspecific interactions were identified using a similar stable cell line expressing EphB2 and FLAG-tagged GFP (GFP$^+$EphB2$^+$). We found that adaptor proteins Nck1 and Nck2, the Ras GTPase-activating protein p120-RasGAP (RasGAP), and the α- and β-chimaerin RAC GAPs were enriched in Shb immunoprecipitate from cells stimulated with cross-linked ephrinB1 for 1 h (Table 1). The EphB2 receptor was also present but did not reliably demonstrate signaling-dependent association, suggesting that this interaction is weak, transient, or indirect in nature. Chimaerins are expressed in two main isoforms, with and without an SH2 domain. The peptide spectrum of β-chimaerin indicated that the SH2-containing isoform co-precipitated with Shb.

These MS results suggested that Shb forms a functional complex with Nck and RasGAP, both of which have been implicated in EphB2 signaling (20, 21). To further investigate whether Shb forms a complex with Nck and RasGAP following EphB2 activation, we monitored the kinetics of interaction by Western blotting (Fig. 3*A*). Although a low level of RasGAP appeared to associate with Shb prior to ephrinB1 stimulation, the levels of both Nck/Shb and RasGAP/Shb complex formation rose dramatically over the 60-min time period monitored. This pattern of association mirrored the enhancement of Shb tyrosine phosphorylation in Fig. 2. All subsequent experiments used a fixed 1-h time point to examine Shb complexes because this time point gave the strongest response in both assays. Reciprocal immunoprecipitation/Western blots performed on stimulated and unstimulated Shb$^+$EphB2$^+$ and GFP$^+$EphB2$^+$ cells further demonstrated association with Nck (Fig. 3*B*) and RasGAP (Fig. 3*C*), with detectable levels of Shb found only in samples from stimulated cells. Collectively, these results show the induction of a Shb complex with Nck and RasGAP following EphB2 stimulation.

To confirm that Shb interacts with the Chimaerins downstream of EphB2, we examined Shb and Chimaerin immunoprecipitates in the context of EphB2 signaling. GFP$^+$EphB2$^+$ and Shb$^+$EphB2$^+$ cells expressing YFP-tagged[3] α-Chimaerin or YFP-tagged β-Chimaerin were stimulated with ephrinB1. The presence of YFP-Chimaerin and FLAG-Shb was analyzed by Western blotting following immunoprecipitation with anti-FLAG (Fig. 4*A*) or anti-YFP specific antibodies (Fig. 4*B*). FLAG-tagged Shb immunoprecipitates contained both α- and β-Chimaerin, specifically in samples from ephrinB1-stimulated cells. Chimaerins were not detected in FLAG-tagged GFP control precipitates. The reverse immunoprecipitation of YFP, YFP–α-Chimaerin, and YFP–β-Chimaerin similarly demonstrated an association between Shb and the Chimaerins (Fig. 4*B*). FLAG-

[3] The abbreviations used are: YFP, yellow fluorescent protein; siShb, siRNA targeting Shb; CST, cortical spinal tract.

Table 1
Mass spectrometry analysis of FLAG-tagged Shb immunoprecipitation

		Experiment 1						Experiment 2					
		Stimulated			Unstimulated			Stimulated			Unstimulated		
NCBI	Protein	Total peptides	Unique peptides	Mascot score	Total peptides	Unique peptides	Mascot score	Total peptides	Unique peptides	Mascot score	Total peptides	Unique peptides	Mascot score
gi106879210	Shb	2568	131	1429	2191	115	9330	643	39	2756	645	43	2958
gi5453754	Nck1	18	12	665				28	5	548			
gi52630423	Nck2	10	4	320				17	2	459			
gi4506431	RasGAP	143	32	2250				47	3	1082	2	2	75
gi209364623	α-Chimaerin	11	6	415				9	2	358			
gi21396504	EphB2	8	6	344				6	8	322	6	6	247
gi150378533	Deubiquitinating enzyme 7	6	6	245	3	3	108	4	2	141			
gi4757980	β-Chimaerin	3	2	76				2	3	98			
gi102469034	Janus kinase 1	2	2	85							3	3	167
gi124378039	SEC16 homolog A	2	2	93							2	2	69

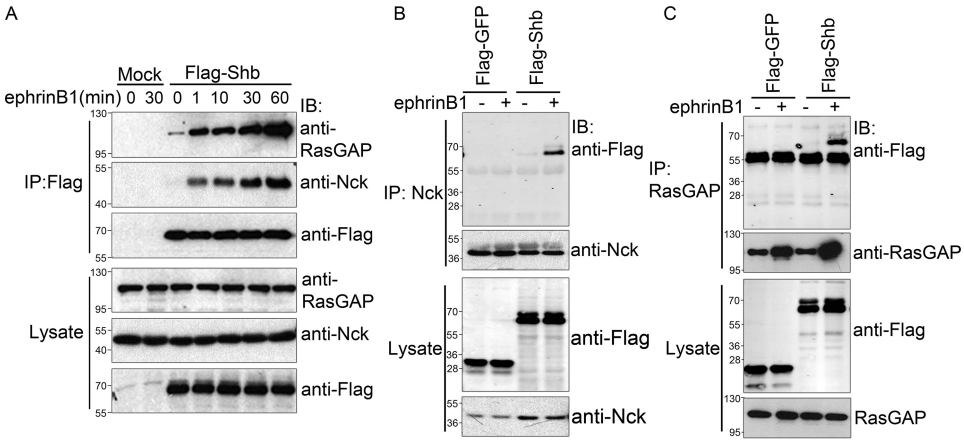

Figure 3. Shb interacts with RasGAP and Nck following EphB2 activation. EphB2$^+$ HEK293 expressing FLAG-tagged GFP or FLAG-tagged Shb were stimulated with soluble, cross-linked ephrinB1. *A*, Western blotting analysis of RasGAP, Nck, FLAG-Shb, and FLAG-GFP in cell lysate and immunoprecipitates of FLAG. *B*, Western blotting analysis of FLAG-GFP, FLAG-Shb, and Nck in anti-Nck precipitates. *C*, Western blotting analysis of FLAG-GFP, FLAG-Shb, and RasGAP in anti-RasGAP immunoprecipitates. Molecular mass (kDa) is indicated to the *left* of each panel. *IP*, immunoprecipitation; *IB*, immunoblotting.

Shb was enriched in precipitates of YFP-Chimaerin from stimulated EphB2$^+$ cells. These data indicate that EphB2 stimulation enhances the association between Shb and Chimaerins.

Nck, RasGAP, and the Chimaerins all contain SH2 domains capable of interacting directly with phosphorylated tyrosines in Shb. We previously reported significantly enhanced Shb phosphorylation on tyrosines 114, 246, 268, 297, and 336 in EphB2$^+$ cells stimulated by ephrinB1$^+$ cells (13). To test whether these residues contribute to interactions with candidate SH2-containing proteins, we generated a series of variants in which each individual tyrosine was mutated to phenylalanine. Additionally, we created Y268F/Y336F Shb double mutant as RasGAP binds to similar phosphotyrosine motifs in the DOK1 scaffold (*2F* in Fig. 5*A*) (22). We then monitored the efficiency of protein association with each Shb variant following EphB2 stimulation. The Shb mutant Y297F demonstrated impaired Nck binding (Fig. 5*B*), whereas the Shb Y246F mutant exhibited diminished RasGAP binding (Fig. 5*C*). Mutation of Shb Tyr^{336} ablated binding of both α- and β-chimaerins (Fig. 6). These data demonstrate that distinct phosphotyrosine sites on Shb mediate the binding of distinct SH2-signaling proteins.

We next investigated whether the SH2 domains of RasGAP and α-Chimaerins were sufficient to mediate the interaction with Shb. (Fig. 7). We observed that the expressed GST-α-Chimaerin SH2 domain precipitated WT Shb efficiently from the lysates of stimulated cells and that this construct exhibited reduced binding to the Shb Y336F mutant (Fig. 7*A*). We observed that the C-terminal SH2 domain of RasGAP (C-SH2) was sufficient to bind to Shb (Fig. 7*B*), and interaction was lost with the Shb Y246F mutant. In distinction, the N-terminal SH2 domain of RasGAP (N-SH2) demonstrated no interaction with Shb. We note, however, that the RasGAP N-SH2 construct was difficult to express, suggesting that this construct may not be fully functional. These data indicate that the α-Chimaerin SH2 and the C-terminal SH2 of RasGAP effectively interact with Shb Tyr^{336} and Tyr^{246}, respectively.

To determine the functional significance of these interactions during EphB2–ephrinB1 boundary formation, we constructed a GFP$^+$EphB2$^+$ cell line expressing a Shb mutant with phenylalanine mutations at Tyr^{246}, Tyr^{297}, and Tyr^{336} (3FShbR). Four silent nucleotide mutations were also introduced for siRNA resistance, which would allow for testing of mutant activity in the absence of endogenous Shb. Control cell lines expressed vector alone, WT Shb (Shbwt), and an siRNA-resistant WT Shb (ShbR). Untreated cell lines were initially characterized for EphB2–ephrinB1 cell segregation activity by visualization of tightly packed GFP$^+$ cells within a confluent well of a 96-well dish (Fig. 8). Cell lines with enhanced

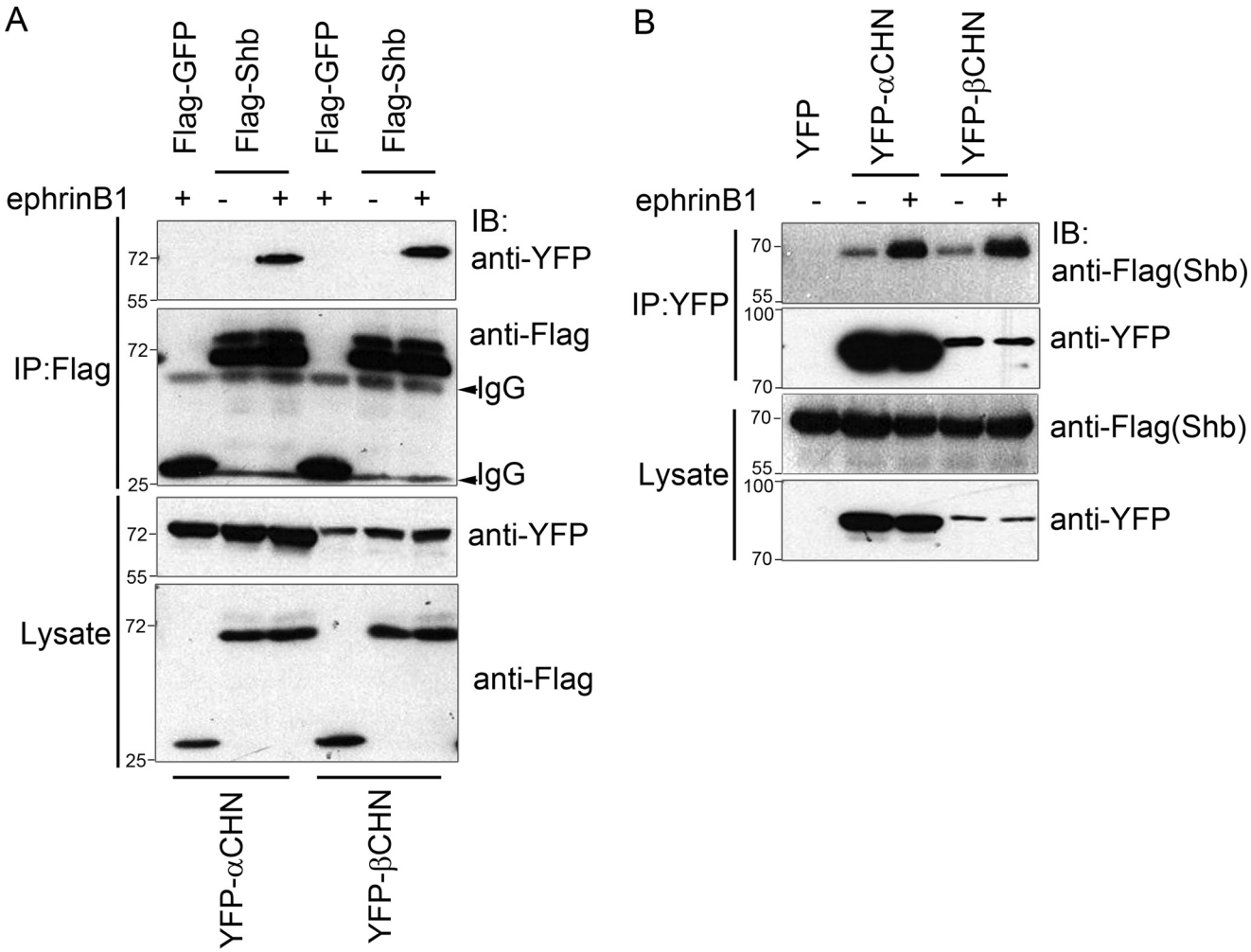

Figure 4. Shb interacts with α-chimaerin and β-chimaerin following EphB2 activation. EphB2$^+$ FLAG-GFP$^+$ HEK293 and EphB2$^+$ FLAG-Shb$^+$ HEK293 were transfected with YFP-tagged α- or β-chimaerin. The cells were stimulated by ephrinB1 as indicated. *A*, Western blotting analysis of FLAG-GFP, FLAG-Shb, YFP-α-chimaerin, and YFP-β-chimaerin in anti-FLAG precipitates. *B*, Western blotting analysis of YFP, YFP-α-chimaerin, YFP-β-chimaerin, and FLAG-Shb in anti-YFP immunoprecipitates. Molecular mass (kDa) is indicated to the *left* of each panel.

expression of WT Shb, Shbwt, and ShbR, formed more compact clusters with sharper borders compared with 3FShbR cells, the parental cell line and vector control (Fig. 8*A*). This effect was apparent in co-cultures with HEK293 cells (−ephrinB1), which express low levels of endogenous ephrinB ligands (23), and was further enhanced during co-cultures with ephrinB1$^+$ cells (+ephrinB1). Increased compaction was measurable as a decreased cluster size and enhanced fluorescence in Shb and ShbR samples (Fig. 8, *B* and *C*). Similar trends with statistical significance were apparent upon a manual count of efficient GFP$^+$ cell segregation marked by clusters with an elevated center and smooth, rounded borders (Fig. S2). The ability of WT Shb to support boundary formation in the absence of exogenous ephrinB ligand was also seen during routine cell culture, where the Shb and ShbR cells spontaneously formed tight clusters that were slightly elevated from the cell monolayer (Fig. S3). Collectively, these data show that WT Shb is sufficient to enhance EphB2-mediated boundary formation, whereas the 3FShb is not.

Shb was then depleted by siRNA to allow for examination of WT ShbR and 3FShbR activity in the absence of endogenous Shb (Fig. 9*A*). Segregation of EphB2$^+$GFP$^+$ cells expressing vector alone and Shbwt was impaired when siRNA targeting Shb (siShb) was added to the co-culture (Fig. 9, *B–D*, and Fig. S4). Expression of WT, siRNA-resistant ShbR partially restored the formation of tight GFP$^+$ clusters during siShb treatment, whereas 3FShbR cells had a phenotype similar to that of Shbwt and vector controls. Thus, the 3F mutation ablates any restorative function, suggesting that these tyrosines are required for Shb activity during EphB2–eprhinB1 cell sorting.

Because RasGAP (21, 24, 25), Nck (21, 26), and α-Chimaerin (26–30) constitute the signaling components of several Eph receptor pathways, we examined the role of Shb in mediating Eph receptor signaling. HEK293 cells were transiently transfected to express EphA8, EphA4, or EphB4 together with Myc-tagged Shb. Cells expressing EphA and EphB receptors were stimulated with ephrinA1 and ephrinB1, respectively. Immunoprecipitation of Shb, and Western blotting analysis with anti-phosphotyrosine, anti-RasGAP, and anti-Nck was then used to assess the phosphorylation and scaffold function of Shb (Fig. 10). Anti-phosphotyrosine analysis of cell lysates demonstrated the presence of a high-molecular-mass phosphoprotein (>100 kDa) consistent with the activated Eph receptor. Transient overexpression of the Eph receptors is sufficient to induce

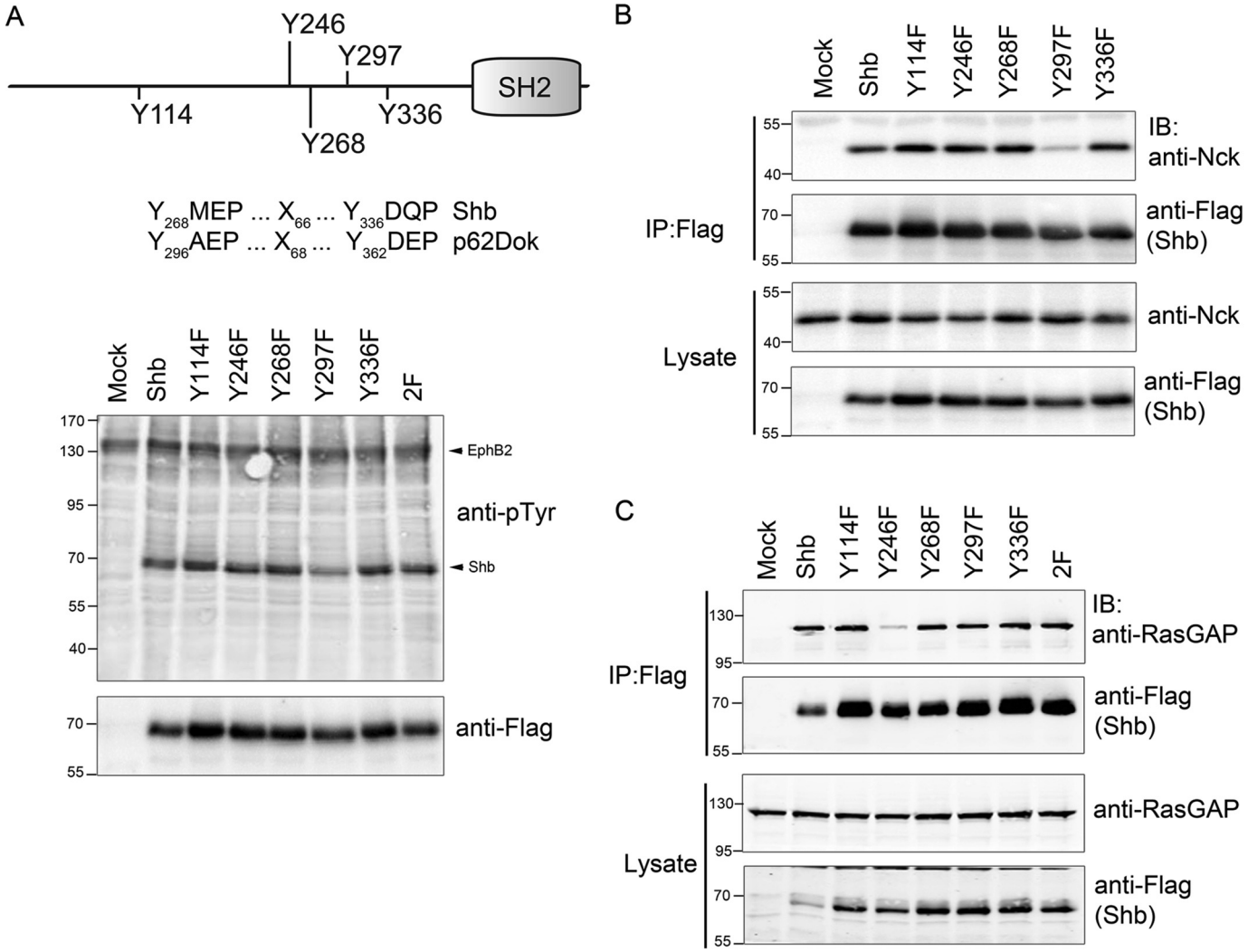

Figure 5. Shb requires Tyr^{246} and Tyr^{297} to bind RasGAP and Nck, respectively. Shb was mutated at tyrosine residues previously shown to be phosphorylated during EphB2 signaling (13). EphB2^{+} HEK293 cells were transfected with empty vector, FLAG-tagged Shb, and FLAG-tagged Shb mutants. The cells were stimulated with cross-linked ephrinB1. *A*, diagram of tyrosines targeted for mutation in Shb, including one double mutation of sites that resemble the RasGAP SH2-binding motifs reported for the p62Dok scaffold (22). Total phosphorylation and expression are shown by Western blotting. *B* and *C*, immunoprecipitates of FLAG were analyzed by Western blotting using either anti-Nck (*B*) or anti-RasGAP (*C*) antibodies. Molecular mass (kDa) is indicated to the *left* of each panel. *IP*, immunoprecipitation; *IB*, immunoblotting.

transphosphorylation of the receptors in the absence of ephrin ligand (31–33). EphA4 exhibited enhanced activation following stimulation, as indicated by the induction of a high-molecular-mass phosphotyrosine protein. Each active receptor was capable of inducing Shb tyrosine phosphorylation and the induction of Shb complexes with Nck and RasGAP. These results demonstrate that Shb acts as a scaffold for RasGAP and Nck downstream of multiple Eph receptors.

Discussion

Eph receptors play a major role in generating and maintaining distinct tissue boundaries and regional segregation of specific cell types within a tissue. Restricted mingling of cells and the formation of distinct borders is controlled through differences in cell adhesion, repulsion, mobility and the generation of cortical tension (reviewed in Refs. 34 and 35). A current challenge is to define the mechanisms translating Eph receptor tyrosine kinase signaling to polarized motility and cell segregation. In this report, we define Shb as a tyrosine-phosphorylated scaffold protein downstream of Eph receptors and demonstrate that it has an essential role in EphB2-mediated boundary formation.

In a previously characterized Eph receptor- and ephrin-driven segregation model system (23), Shb depletion in the EphB2 cell line affects boundary formation, whereas no apparent change is observed when Shb is absent in the ephrin-B1 cells. This indicates that Shb is not required for ephrin signaling, but an interaction between the EphB2 receptor and Shb is critical to establish and/or maintain the Eph–ephrin borders. Consistent with this interpretation is the observation that activation of the receptor leads to increased Shb tyrosine phosphorylation, indicating that Shb is a substrate of Eph receptors and/or a downstream tyrosine kinase. Furthermore, we found that Shb interacts with Nck, RasGAP, and α- and β-Chimaerin. These latter proteins have been shown to perform molecular

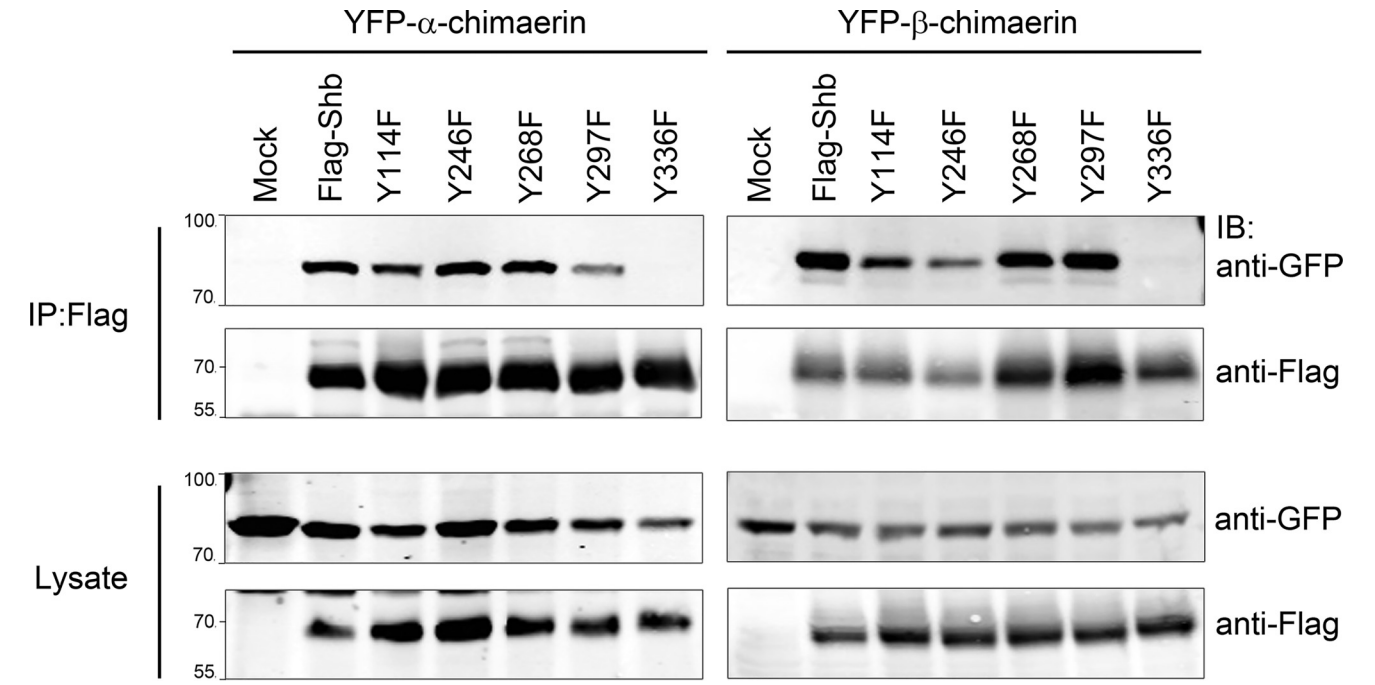

Figure 6. Shb requires Tyr^{336} to bind α- and β-chimaerin. EphB2^{+} HEK293 cells were transfected with empty vector, FLAG-tagged Shb, and FLAG-tagged Shb mutants, as well as α- or β-chimaerin as indicated. The cells were stimulated with cross-linked ephrinB1. Anti-FLAG precipitates were analyzed for the presence of YFP-α-chimaerin and YFP-β-chimaerin by Western blotting. Molecular mass (kDa) is indicated to the *left* of each panel. *IP*, immunoprecipitation; *IB*, immunoblotting.

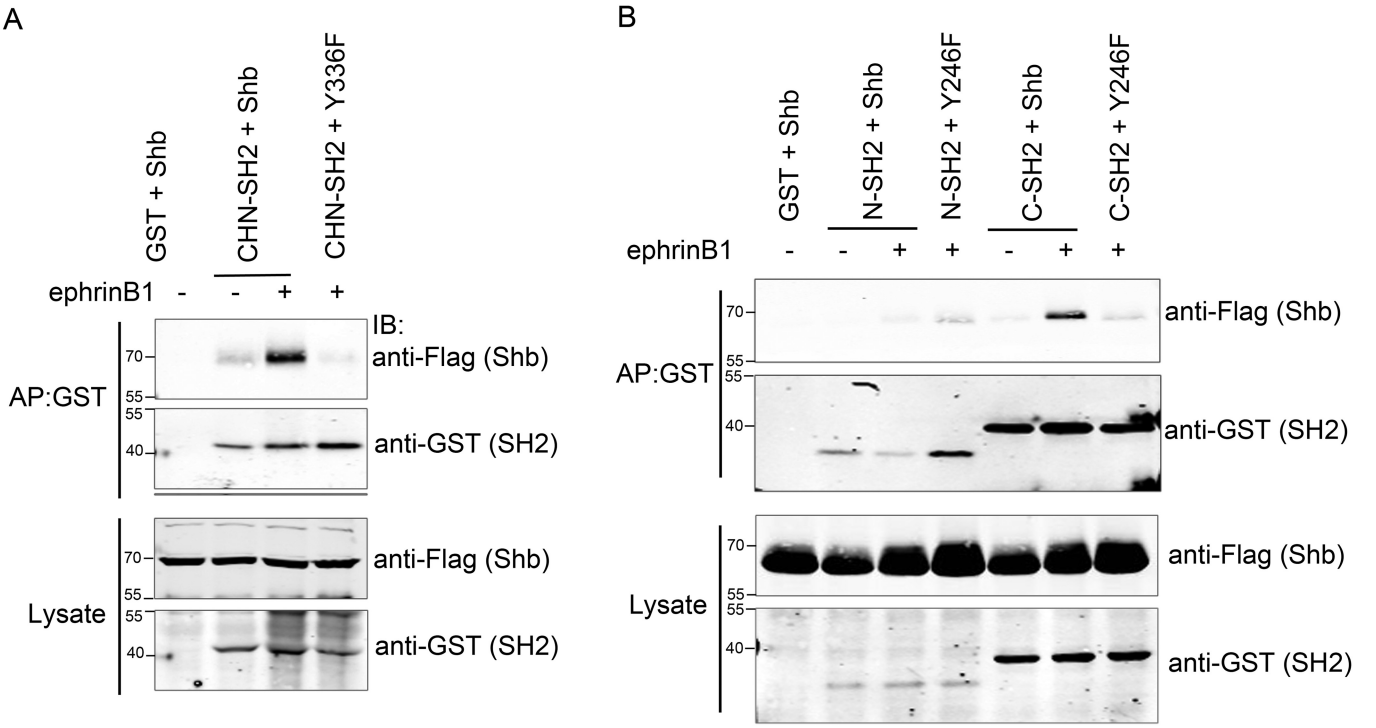

Figure 7. Shb binds the SH2 domains of α-chimaerin and RasGAP. EphB2^{+} HEK293 cells were transfected with empty vector, GST-tagged SH2 domains, FLAG-tagged Shb, FLAG-tagged Shb Y336F mutant, and FLAG-tagged Shb Y246F mutant as indicated. The cells were treated with cross-linked ephrinB1 or with cross-linking antibody alone. The binding capacity of the SH2 domains from α-chimaerin (*A*) and p120 RasGAP (*B*) were assessed by affinity purification (*AP*) of the GST-tagged domain and Western blotting detection of FLAG-Shb. Molecular mass (kDa) is indicated to the *left* of each panel. *IB*, immunoblotting. *CHN*, chimaerin.

functions that could facilitate cell segregation. Specifically, GAPs, like RasGAP and Chimaerin, are known to control cell movement downstream of Eph receptors through localized inhibition of GTPases (reviewed in Ref. 36) and Nck provides a direct link to the cytoskeleton by binding components of the WASP/Arp2/3 actin remodeling system through its SH3 domains (reviewed in Refs. 37 and 38). These proteins were also found to be required for EphB2–ephrinB1 cell segregation in our previously published siRNA screen (13). Thus, our data are consistent with the notion that Shb plays a key role in coordi-

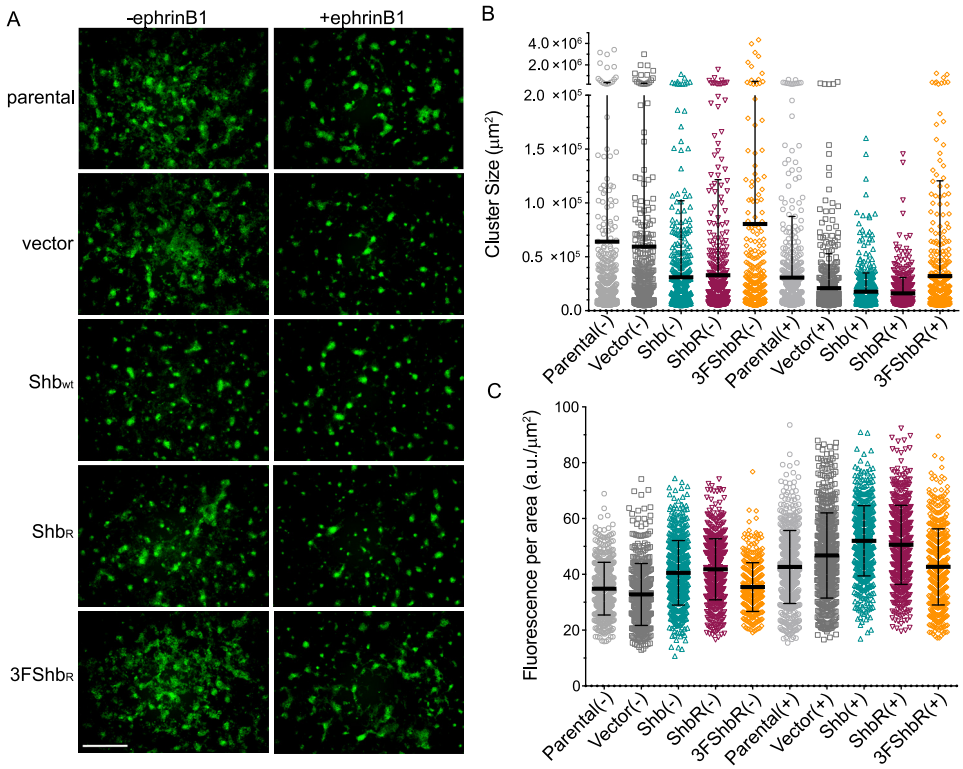

Figure 8. WT Shb enhances EphB2–ephrinB1 cell sorting. EphB2$^+$GFP$^+$ HEK293 cells and derivatives expressing vector, exogenous WT Shb (Shbwt), an siRNA-resistant WT Shb (ShbR), and an siRNA-resistant Y246F/Y297F/Y336F mutant of Shb (3FShbR) were co-incubated with HEK293 (−ephrinB1) or ephrinB1$^+$HEK293 (+ephrinB1). *A*, fluorescent microscopy was used to visualize segregation of the EphB2$^+$GFP$^+$ cells within a confluent monolayer (4× magnification). Confluency was confirmed by automated detection in a differential interference contrast image (data not shown). *Scale bar*, 1000 μm. *B* and *C*, efficient segregation was enumerated for −ephrinB1(−) and +ephrinB1(+) samples as mean cluster size + standard deviation (*B*) and mean fluorescence per area ± standard deviation (*C*) ($n = 8$).

nating Nck, RasGAP, and α- and β-Chimaerin activity during Eph receptor signaling.

Although the Eph receptor does undergo tyrosine autophosphorylation and can act as a scaffold for the binding of SH2-containing signaling proteins, our data show that these interactions are insufficient for cell segregation. Shb provides critical scaffold function through phosphotyrosine- and SH2 domain–mediated interactions. The Shb molecule contains a flexible N-terminal region capable of multiple protein–protein interactions simultaneously. However, previous reports have failed to conclusively define Shb as a scaffold by characterizing functional phosphorylation motifs. We report here the first analysis of Eph receptor–mediated Shb scaffolding and define three functional Shb phosphotyrosine sites, pTyr^{246}, pTyr^{297}, and pTyr^{336}, that bind RasGAP, Nck, and Chimaerin, respectively. Each Shb motif fits the consensus sequence of an EphA4 kinase substrate with acid residues at the +1 or +2 positions and a hydrophobic proline at the +3 position (39). The proline at the +3 position also means that the phosphotyrosine motifs at Tyr^{246} and Tyr^{297} conform to known SH2-binding preferences for RasGAP and Nck, respectively (20, 40). The binding consensus for the Chimaerin SH2 domain has yet to be elucidated. Our data define a direct interaction between Tyr^{336} and the isolated SH2 domain or full-length α- and β-Chimaerin constructs. Furthermore, the importance of the SH2 domain in the Chimaerin–Shb interaction was inferred by the endogenous interactions detected in our MS analysis of Shb precipitates. Peptides unique to both α2- and β2-chimaerin were readily detected following Eph receptor stimulation, whereas natural isoforms of α- and β-chimaerin that lack the SH2 domain (α1 and β1) were not.

We also demonstrate that Shb complexes are generated by multiple Eph receptors, suggesting that the homo- or heteromeric content of the active Eph receptor oligomers will not affect a Shb-directed pathway. Still, there is evidence that cell type–specific or other context-dependent signaling does occur through RasGAP, Nck, and Chimaerin downstream of Eph receptors. For example, each of these Shb interactors have been previously implicated in EphB2- and EphA4-mediated neuronal growth cone collapse (20, 28, 41). In that context, RasGAP and Nck were shown to interact with a distinct scaffold protein, Dok1 (20). Dok1 was not identified as a Shb interactor in our MS analysis. Although indirect interactions between Shb and Dok1 cannot be ruled out, this suggests the use of distinct scaffolds to localize RasGAP and Nck activity for context- or cell type–specific function.

Similarly, EphA4-, Chimaerin-, and Nck-mediated neuronal retraction occurs independent of Shb during cortical spinal tract (CST) development. This is apparent because Chimaerin, Nck, or EphA4 null mice have hopping gait, like that of a rabbit, because of aberrant CST formation (3, 4, 6, 26, 27, 29, 30), whereas Shb null mice lack this readily observable phenotype (42).[4] Thus, Shb is not required for CST formation and

[4] M. Welsh, personal communication.

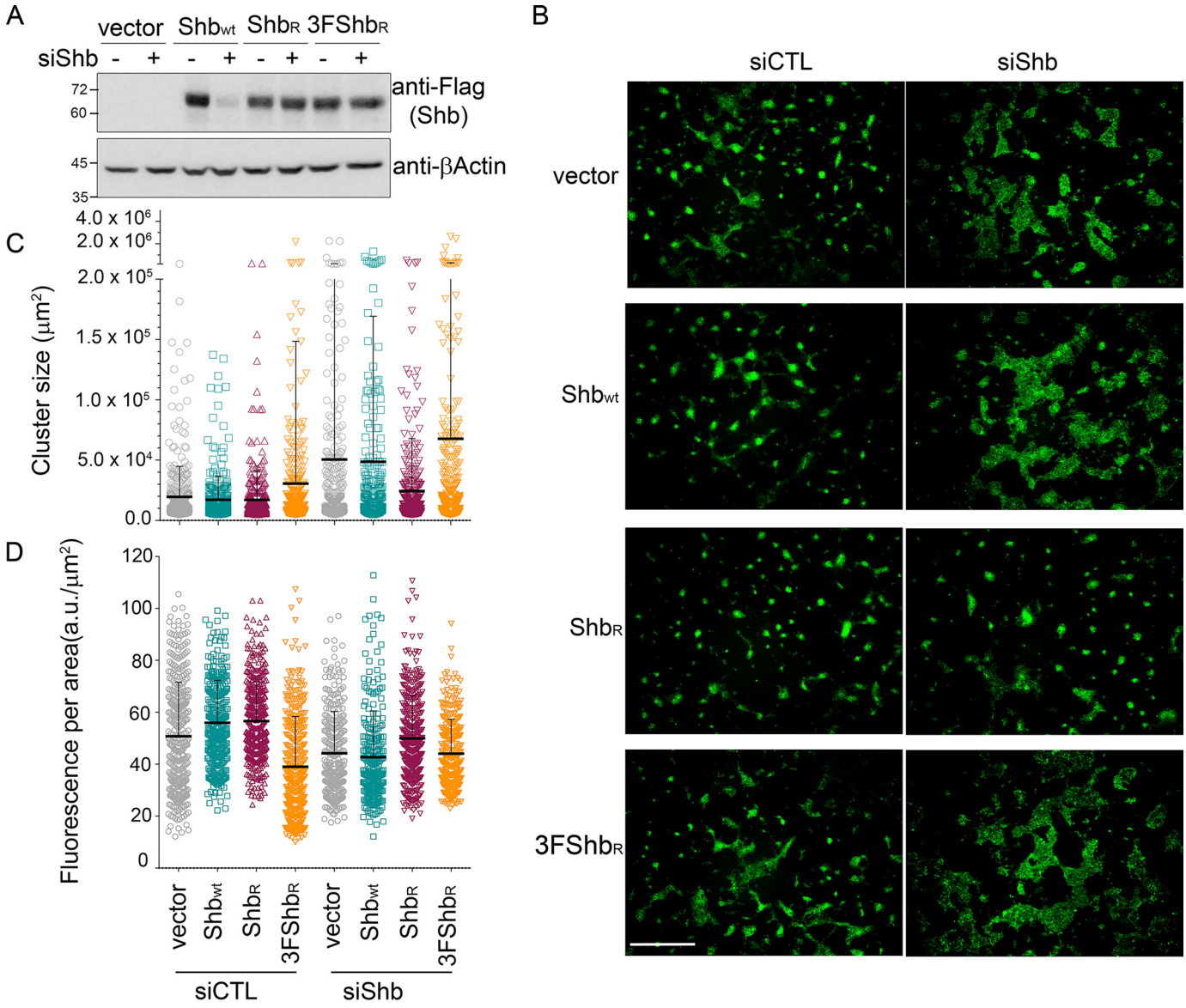

Figure 9. WT Shb compensates for endogenous Shb depletion during EphB2-mediated cell sorting, but 3FShb does not. Shbwt, ShbR, and 3FShbR cell lines were co-incubated with ephrinB1^{+}HEK293 in the presence of control siRNA (*siCTL*) or siRNA directed against Shb (*siShb*). *A*, depletion of FLAG-tagged Shb by siRNA was detected by Western blotting. Molecular mass (kDa) is indicated to the *left* of each panel. *B*, fluorescent microscopy was used to visualize segregation of the GFP^{+} cells within a confluent monolayer (4× magnification). Confluency was confirmed by automated detection in a differential interference contrast image (data not shown). *Scale bar*, 1000 μm. *C*, efficient segregation was enumerated as mean cluster size ± standard deviation. *D*, mean fluorescence per area ± standard deviation ($n = 8$).

is not critical within the EphA4–Chimaerin–Nck pathway in this context. Further investigation is required to determine how Shb and other scaffolds fit into the context-dependent nature of Eph receptor signaling; however, Shb activity may be limited by regionalized expression of Shb RNA, which has been described in mouse embryos (43). Furthermore, the related scaffolds, Shd, She, and Shf, have reasonable conservation of the RasGAP, Nck, and Chimaerin SH2-binding motifs, as well as the spacing between the Nck- and Chimaerin-binding sites (Fig. S5), and may compensate for Shb in some instances.

Overall, our data demonstrate that Shb acts as a tyrosine-phosphorylated scaffold downstream of EphB2 and performs an essential function in directed cell movement. Furthermore, the assembly of Shb in similar complexes downstream of EphA4, EphA8, and EphB4 suggests that this scaffold orchestrates a signaling module conserved among multiple Eph receptors. Although additional scaffolds and adaptors will contribute to the sophisticated ability of Eph receptors to generate and maintain tissue boundaries, our results begin to clarify the phosphotyrosine-mediated signaling events that translate to heterotypic cell segregation.

Experimental procedures

Plasmids

PCR was used to amplify Shb (NM_003028, amino acids 2–509); β-chimaerin (BC112155, 469 amino acids); α-chimaerin (DQ890613, 459 amino acids) α-chimaerin SH2 domain (amino acids 13–178); RasGAP (BC033015) N-SH2 domain

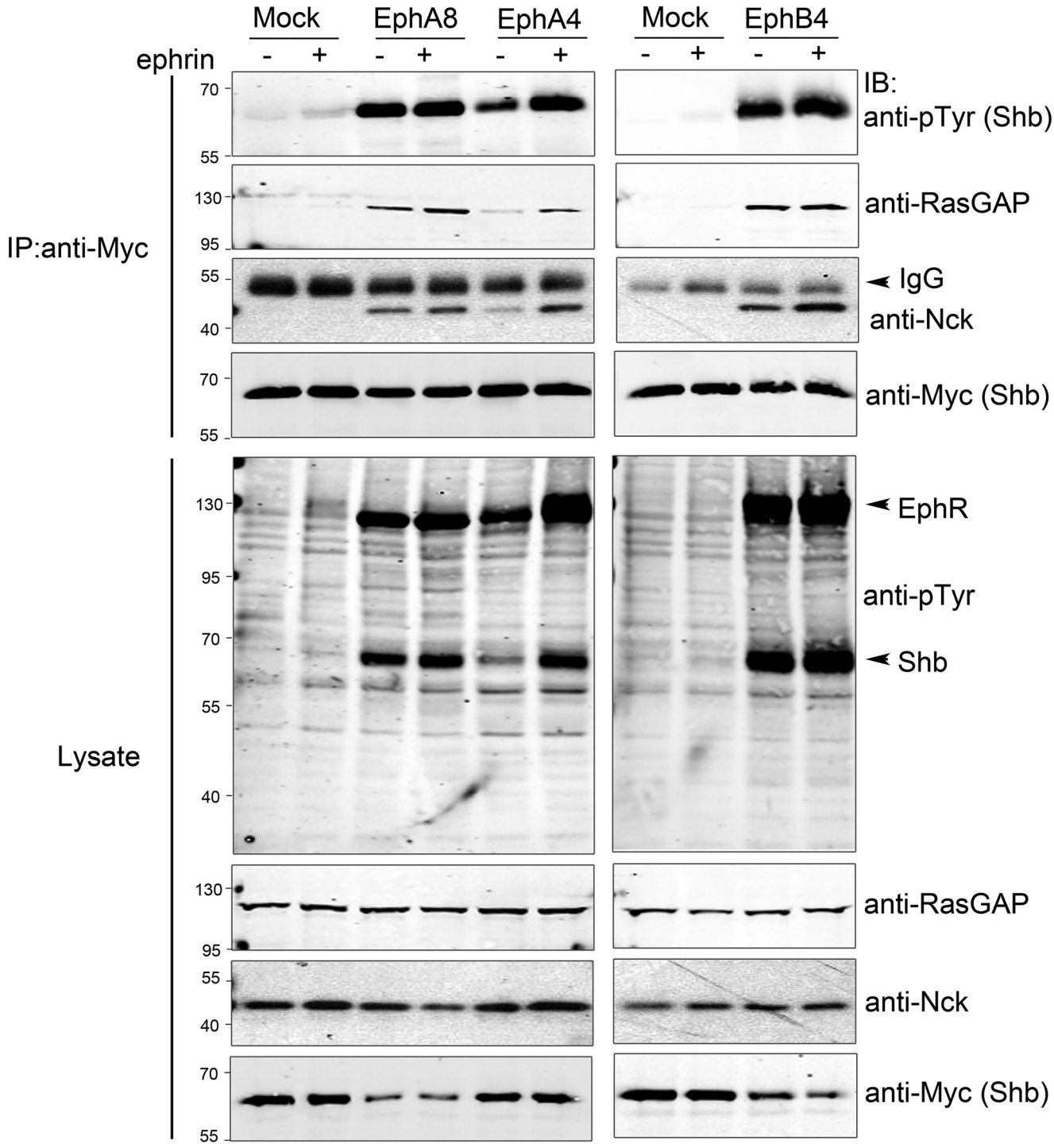

Figure 10. Shb is tyrosine-phosphorylated and interacts with Nck and RasGAP downstream of active EphA4, EphA8, and EphB4. HEK293 cells were transfected with Myc-tagged Shb and either an empty vector or a FLAG-tagged Eph receptor. EphA4- and EphA8-expressing cells were stimulated with cross-linked ephrinA1, and EphB4-expressing cells were stimulated with ephrinB1. Immunoprecipitates of Myc-Shb were analyzed by Western blotting using anti-phosphotyrosine, anti-RasGAP, anti-Nck, and anti-Myc. Molecular mass (kDa) is indicated to the *left* of each panel. *IP*, immunoprecipitation; *IB*, immunoblotting.

(amino acids 173–280); and C-SH2 domain (amino acids 342–470). Each cDNA was digested by AscI (5′) and PacI (3′). Shb cDNA was inserted into V179 pLP Triple FLAG for transient expression. For stable expression, Shb or a FLAG-tagged Shb was inserted into and V207 pRetro-Triple FLAG S.D. or pMXs IRES puro, respectively. Full-length β-chimaerin and α-chimaerin sequences were expressed in V3522 pLP-mCitrine C1 and pLP-mCitrine C1 SD, respectively. The SH2 cDNA of α-chimaerin, RasGAP N-SH2, and RasGAP C-SH2 were cloned into the GST-fusion protein mammalian-expression vector pEBG. All vectors were authenticated through DNA sequencing and protein expression assays. Lipofectamine 2000 (Invitrogen) was used according to the manufacturer's protocol for vector transfection.

Cell culture

HEK293 cells stably expressing ephrinB1 or myristoylated GFP and EphB2 have been described previously (23). Polyclonal populations of EphB2$^+$ HEK293 cells stably expressing a FLAG-tagged GFP or a FLAG-tagged Shb were generated by serial passaging and selection in puromycin-containing media.

EphB2 stimulation

EphB2$^+$ HEK293 were serum-starved overnight in 1%FBS. EphrinB1 Fc Chimera (R&D Systems) was cross-linked by goat anti-human IgG and then incubated with the cells at a concentration of 2 μg/ml for 1 h unless otherwise specified.

Immunoprecipitation, GST affinity purification, and Western blotting

The cells were lysed on ice in Nonidet P-40 lysis buffer (50 mM Tris-HCl, pH 7.4, 1% Nonidet P-40, 0.25% sodium deoxycholate, 150 mM NaCl, 1 mM EGTA, 10 mM NaF, 10 mM β-glycerol phosphate, 1 mM Na_3VO_4, 10 μg/ml pepstatin, 100 μg/ml leupeptin, 100 μg/ml aprotinin). Lysates were processed at 4 °C during affinity purification. The proteins were immunoprecipitated or affinity-purified with Pierce GSH–agarose (ThermoScientific) for 1–2 h and then washed three times with lysis buffer. Western blotting analysis was performed according to standard protocols. Anti-FLAG (M2, Sigma–Aldrich), anti-c-Myc (C3956, Sigma–Aldrich), anti-RasGAP (B4F8, Santa Cruz Biotechnology Inc.), anti-GFP (ab290, Abcam), and anti-phosphotyrosine (4G10, Merck Millipore) were used for immunoprecipitation and Western blotting. Polyclonal anti-Nck (3 × 3), which recognizes the three SH3 domains of Nck1 and Nck2 as previously described (44), was also used for immunoprecipitation and Western blotting.

Mass spectrometry

Affinity-purified proteins were eluted with 3% phosphoric acid and processed as described previously (45). Briefly, eluates were equilibrated prior to loading and washed with 10 mM potassium phosphate buffer, pH 3, in a TopTip column (Glygen Co.) packed with 30-μm SCX beads (PolyLC Inc.). Bound proteins were reduced with tris(2-carboxyethyl)phosphine (Sigma–Aldrich) then alkylated and digested for 1–2 h in a trypsin solution (2 mg/ml sequencing grade porcine trypsin (Promega), 100 mM Tris, 10 mM iodoacetamide, pH 8). Peptides were eluted in 200 μM NH_4HCO_3, pH 8, acidified with 0.03% formic acid. All data were acquired on a TripleTOF 5600 instrument (AB Sciex) equipped with a NanoLC-Ultra 1D plus system (Eksigent). The instrument was set to run an information-dependent acquisition method consisting of an MS1 TOF scan from 400 to 1300 Da with an accumulation time of 250 ms, followed by 20 candidate ion MS2 scans (50 ms each) set between 100 and 1250 Da. The samples were loaded onto a cHiP-LC column 75 μm × 15 cm (Eksigent) packed with ReproSil-Pur 3 μm C18-AQ (Dr. Maisch HPLC GmbH) and analyzed using a 90-min gradient from 5–35% acetonitrile with 0.1% formic acid, at a flow rate of 250 nl/min.

All raw files were converted to mgf format using ProteinPilot software, and MS/MS spectra were analyzed using Mascot (Matrix Science) and ProHits. Mascot searched against human proteins from the ENSEMBL database (46,768 entries) with the following parameters: carbamidomethyl (C) was set as a fixed modification; deamidated (NQ), oxidation (M), phospho-Tyr, and phospho-Ser/Thr were set as variable modifications; and two missed trypsin cleavages were allowed. Precursor mass tolerance was 12 ppm, and MS/MS mass accuracy was 0.6 Da. Mass spectrometry data were stored, searched, and analyzed using the ProHits laboratory information management system platform (46). Prohits biofilters were set to exclude keratin, ribonucleoprotein, histone, translation elongation factors, albumin, DEAD/H box, ribosomal, and heat shock proteins.

Plasmid mutagenesis

Shb cDNA within the pLP Triple FLAG plasmid was mutagenized by PCR using the QuikChange Lightning site-directed mutagenesis kit (Agilent) or *Pfu* Turbo DNA polymerase (Agilent Technologies). The buffer supplied by the manufacturer was supplemented with 10% QuikSolution or DMSO, respectively. PCR cycling was performed according to standard protocols.

siRNA

Shb siRNA (Dharmacon, GE Healthcare) treatments were performed using Lipofectamine RNAiMax (Invitrogen). Selective depletion in EphB2$^+$GFP$^+$ or ephrinB1$^+$ HEK293 was performed with a pool of four siRNA, 48 h prior to replating for the cell sorting assay (Fig. 1) and achieved average efficiencies of 86.3 ± 2.9 and 73.8 ± 2.4%, respectively. For rescue of Shb function (Figs. 8 and 9), a single Shb siRNA (Dharmacon, GE Healthcare, D-019715–18) with average efficiencies of 92.0 ± 1.5 and 92.0 ± 2.4% in EphB2$^+$GFP$^+$ and ephrinB1$^+$ HEK293, respectively, was added directly to both cell types in the segregation assay.

Cell segregation assay

EphB2$^+$ HEK293 expressing EphB2 and a membrane-localized GFP were mixed at a 1:1 ratio with HEK293 or HEK293 expressing ephrinB1 following collection in an enzyme-free cell dissociation buffer (Gibco). The cells were seeded at a density that allowed for approximately 2–3 days of proliferation. Imaging of sorted cells took place at 100% confluency. The cells were imaged live (Figs. 8 and 9) or fixed with 4% paraformaldehyde (Sigma–Aldrich) for nuclear staining with Hoescht (Invitrogen) (Fig. 1). Clusters of GFP$^+$EphB2$^+$ HEK293 were visualized using the IncuCyte live cell analysis system (Essen Bioscience Inc.) or the Leica DMIRE2 microscope, with a Hamamatsu ORCA charge-coupled device camera and Volocity image capture software (Improvision). Quantitation of segregated GFP$^+$ clusters was performed manually on groups of GFP$^+$ cells with an area greater than 2500 μm^2. Requisite features of a positive cluster included formation of a smooth boundary with few GFP$^+$ membrane projections toward the GFP$^-$ cells and the angling of GFP$^+$ cells toward an elevated point or line of symmetry in the center of the cluster. Statistical differences were determined by a nested *t* test. Cluster size and relative fluorescence intensity was analyzed using ImageJ software (National Institute of Health) and a minimal size of 5000 μm^2.

Author contributions—M. J. W. and R. R. conceptualization; M. J. W. formal analysis; M. J. W., M. S. H., and G. D. G. investigation; M. J. W., M. S. H., G. D. G., R. D. B., M. A. S., C. J., and M. T. methodology; M. J. W., M. S. H., G. D. G., and R. D. B. writing-original draft; M. J. W. writing-review and editing; S. A. D. software; R. R. supervision.

Acknowledgments—We thank Dr. Tony Pawson for intellectual contribution and funding he provided as the initial supervisor of this project. We also thank Geraldine Mbamalu and Jose La Rose for technical support.

References

1. Kania, A., and Klein, R. (2016) Mechanisms of ephrin–Eph signalling in development, physiology and disease. *Nat. Rev. Mol. Cell Biol.* **17,** 240–256 CrossRef Medline
2. Batlle, E., Henderson, J. T., Beghtel, H., van den Born, M. M., Sancho, E., Huls, G., Meeldijk, J., Robertson, J., van de Wetering, M., Pawson, T., and Clevers, H. (2002) β-Catenin and TCF mediate cell positioning in the intestinal epithelium by controlling the expression of EphB/ephrinB. *Cell* **111,** 251–263 CrossRef Medline
3. Dottori, M., Hartley, L., Galea, M., Paxinos, G., Polizzotto, M., Kilpatrick, T., Bartlett, P. F., Murphy, M., Köntgen, F., and Boyd, A. W. (1998) EphA4 (Sek1) receptor tyrosine kinase is required for the development of the corticospinal tract. *Proc. Natl. Acad. Sci. U.S.A.* **95,** 13248–13253 CrossRef Medline
4. Kullander, K., Butt, S. J., Lebret, J. M., Lundfald, L., Restrepo, C. E., Rydström, A., Klein, R., and Kiehn, O. (2003) Role of EphA4 and EphrinB3 in local neuronal circuits that control walking. *Science* **299,** 1889–1892 CrossRef Medline
5. Kullander, K., Croll, S. D., Zimmer, M., Pan, L., McClain, J., Hughes, V., Zabski, S., DeChiara, T. M., Klein, R., Yancopoulos, G. D., and Gale, N. W. (2001) Ephrin-B3 is the midline barrier that prevents corticospinal tract axons from recrossing, allowing for unilateral motor control. *Genes Dev.* **15,** 877–888 CrossRef Medline
6. Kullander, K., Mather, N. K., Diella, F., Dottori, M., Boyd, A. W., and Klein, R. (2001) Kinase-dependent and kinase-independent functions of EphA4 receptors in major axon tract formation *in vivo*. *Neuron* **29,** 73–84 CrossRef Medline
7. Yokoyama, N., Romero, M. I., Cowan, C. A., Galvan, P., Helmbacher, F., Charnay, P., Parada, L. F., and Henkemeyer, M. (2001) Forward signaling mediated by ephrin-B3 prevents contralateral corticospinal axons from recrossing the spinal cord midline. *Neuron* **29,** 85–97 CrossRef Medline
8. Boyd, A. W., Bartlett, P. F., and Lackmann, M. (2014) Therapeutic targeting of EPH receptors and their ligands. *Nat. Rev. Drug. Discov.* **13,** 39–62 CrossRef Medline
9. Himanen, J. P., Yermekbayeva, L., Janes, P. W., Walker, J. R., Xu, K., Atapattu, L., Rajashankar, K. R., Mensinga, A., Lackmann, M., Nikolov, D. B., and Dhe-Paganon, S. (2010) Architecture of Eph receptor clusters. *Proc. Natl. Acad. Sci. U.S.A.* **107,** 10860–10865 CrossRef Medline
10. Himanen, J. P., Rajashankar, K. R., Lackmann, M., Cowan, C. A., Henkemeyer, M., and Nikolov, D. B. (2001) Crystal structure of an Eph receptor-ephrin complex. *Nature* **414,** 933–938 CrossRef Medline
11. Wimmer-Kleikamp, S. H., Janes, P. W., Squire, A., Bastiaens, P. I., and Lackmann, M. (2004) Recruitment of Eph receptors into signaling clusters does not require ephrin contact. *J. Cell Biol.* **164,** 661–666 CrossRef Medline
12. Janes, P. W., Griesshaber, B., Atapattu, L., Nievergall, E., Hii, L. L., Mensinga, A., Chheang, C., Day, B. W., Boyd, A. W., Bastiaens, P. I., Jørgensen, C., Pawson, T., and Lackmann, M. (2011) Eph receptor function is modulated by heterooligomerization of A and B type Eph receptors. *J. Cell Biol.* **195,** 1033–1045 CrossRef Medline
13. Jørgensen, C., Sherman, A., Chen, G. I., Pasculescu, A., Poliakov, A., Hsiung, M., Larsen, B., Wilkinson, D. G., Linding, R., and Pawson, T. (2009) Cell-specific information processing in segregating populations of Eph receptor ephrin-expressing cells. *Science* **326,** 1502–1509 CrossRef Medline
14. Obenauer, J. C., Cantley, L. C., and Yaffe, M. B. (2003) Scansite 2.0: Proteome-wide prediction of cell signaling interactions using short sequence motifs. *Nucleic Acids Res.* **31,** 3635–3641 CrossRef Medline
15. Finn, R. D., Bateman, A., Clements, J., Coggill, P., Eberhardt, R. Y., Eddy, S. R., Heger, A., Hetherington, K., Holm, L., Mistry, J., Sonnhammer, E. L., Tate, J., and Punta, M. (2014) Pfam: the protein families database. *Nucleic Acids Res.* **42,** D222–D230 CrossRef Medline
16. Hornbeck, P. V., Kornhauser, J. M., Tkachev, S., Zhang, B., Skrzypek, E., Murray, B., Latham, V., and Sullivan, M. (2012) PhosphoSitePlus: a comprehensive resource for investigating the structure and function of experimentally determined post-translational modifications in man and mouse. *Nucleic Acids Res.* **40,** D261–D270 CrossRef Medline
17. Lindholm, C. K., Gylfe, E., Zhang, W., Samelson, L. E., and Welsh, M. (1999) Requirement of the Src homology 2 domain protein Shb for T cell receptor–dependent activation of the interleukin-2 gene nuclear factor for activation of T cells element in Jurkat T cells. *J. Biol. Chem.* **274,** 28050–28057 CrossRef Medline
18. Holmqvist, K., Cross, M., Riley, D., and Welsh, M. (2003) The Shb adaptor protein causes Src-dependent cell spreading and activation of focal adhesion kinase in murine brain endothelial cells. *Cell Signal.* **15,** 171–179 CrossRef Medline
19. Matskova, L. V., Helmstetter, C., Ingham, R. J., Gish, G., Lindholm, C. K., Ernberg, I., Pawson, T., and Winberg, G. (2007) The Shb signalling scaffold binds to and regulates constitutive signals from the Epstein–Barr virus LMP2A membrane protein. *Oncogene* **26,** 4908–4917 CrossRef Medline
20. Holland, S. J., Gale, N. W., Gish, G. D., Roth, R. A., Songyang, Z., Cantley, L. C., Henkemeyer, M., Yancopoulos, G. D., and Pawson, T. (1997) Juxtamembrane tyrosine residues couple the Eph family receptor EphB2/Nuk to specific SH2 domain proteins in neuronal cells. *EMBO J.* **16,** 3877–3888 CrossRef Medline
21. Becker, E., Huynh-Do, U., Holland, S., Pawson, T., Daniel, T. O., and Skolnik, E. Y. (2000) Nck-interacting Ste20 kinase couples Eph receptors to c-Jun N-terminal kinase and integrin activation. *Mol. Cell Biol.* **20,** 1537–1545 CrossRef Medline
22. Shah, K., and Shokat, K. M. (2002) A chemical genetic screen for direct v-Src substrates reveals ordered assembly of a retrograde signaling pathway. *Chem. Biol.* **9,** 35–47 CrossRef Medline
23. Poliakov, A., Cotrina, M. L., Pasini, A., and Wilkinson, D. G. (2008) Regulation of EphB2 activation and cell repulsion by feedback control of the MAPK pathway. *J. Cell Biol.* **183,** 933–947 CrossRef Medline
24. Xiao, Z., Carrasco, R., Kinneer, K., Sabol, D., Jallal, B., Coats, S., and Tice, D. A. (2012) EphB4 promotes or suppresses Ras/MEK/ERK pathway in a context-dependent manner: Implications for EphB4 as a cancer target. *Cancer Biol. Ther.* **13,** 630–637 CrossRef Medline
25. Kim, I., Ryu, Y. S., Kwak, H. J., Ahn, S. Y., Oh, J. L., Yancopoulos, G. D., Gale, N. W., and Koh, G. Y. (2002) EphB ligand, ephrinB2, suppresses the VEGF- and angiopoietin 1-induced Ras/mitogen-activated protein kinase pathway in venous endothelial cells. *FASEB J.* **16,** 1126–1128 CrossRef Medline
26. Fawcett, J. P., Georgiou, J., Ruston, J., Bladt, F., Sherman, A., Warner, N., Saab, B. J., Scott, R., Roder, J. C., and Pawson, T. (2007) Nck adaptor proteins control the organization of neuronal circuits important for walking. *Proc. Natl. Acad. Sci. U.S.A.* **104,** 20973–20978 CrossRef Medline
27. Iwasato, T., Katoh, H., Nishimaru, H., Ishikawa, Y., Inoue, H., Saito, Y. M., Ando, R., Iwama, M., Takahashi, R., Negishi, M., and Itohara, S. (2007) Rac-GAP α-chimerin regulates motor-circuit formation as a key mediator of EphrinB3/EphA4 forward signaling. *Cell* **130,** 742–753 CrossRef Medline
28. Shi, L., Fu, W. Y., Hung, K. W., Porchetta, C., Hall, C., Fu, A. K., and Ip, N. Y. (2007) α2-Chimaerin interacts with EphA4 and regulates EphA4-dependent growth cone collapse. *Proc. Natl. Acad. Sci. U.S.A.* **104,** 16347–16352 CrossRef Medline
29. Beg, A. A., Sommer, J. E., Martin, J. H., and Scheiffele, P. (2007) α2-Chimaerin is an essential EphA4 effector in the assembly of neuronal locomotor circuits. *Neuron* **55,** 768–778 CrossRef Medline

30. Wegmeyer, H., Egea, J., Rabe, N., Gezelius, H., Filosa, A., Enjin, A., Varoqueaux, F., Deininger, K., Schnütgen, F., Brose, N., Klein, R., Kullander, K., and Betz, A. (2007) EphA4-dependent axon guidance is mediated by the RacGAP α2-chimaerin. *Neuron* **55,** 756–767 CrossRef Medline
31. Noren, N. K., Yang, N. Y., Silldorff, M., Mutyala, R., and Pasquale, E. B. (2009) Ephrin-independent regulation of cell substrate adhesion by the EphB4 receptor. *Biochem. J.* **422,** 433–442 CrossRef Medline
32. Zisch, A. H., Stallcup, W. B., Chong, L. D., Dahlin-Huppe, K., Voshol, J., Schachner, M., and Pasquale, E. B. (1997) Tyrosine phosphorylation of L1 family adhesion molecules: implication of the Eph kinase Cek5. *J. Neurosci. Res.* **47,** 655–665 CrossRef Medline
33. Finger, C., Escher, C., and Schneider, D. (2009) The single transmembrane domains of human receptor tyrosine kinases encode self-interactions. *Sci. Signal.* **2,** ra56 Medline
34. Batlle, E., and Wilkinson, D. G. (2012) Molecular mechanisms of cell segregation and boundary formation in development and tumorigenesis. *Cold Spring Harb. Perspect. Biol.* **4,** a008227 Medline
35. Cayuso, J., Xu, Q., and Wilkinson, D. G. (2015) Mechanisms of boundary formation by Eph receptor and ephrin signaling. *Dev. Biol.* **401,** 122–131 CrossRef Medline
36. Lisabeth, E. M., Falivelli, G., and Pasquale, E. B. (2013) Eph receptor signaling and ephrins. *Cold Spring Harb. Perspect. Biol.* **5,** a009159 CrossRef Medline
37. Li, W., Fan, J., and Woodley, D. T. (2001) Nck/Dock: an adapter between cell surface receptors and the actin cytoskeleton. *Oncogene* **20,** 6403–6417 CrossRef Medline
38. Chaki, S. P., and Rivera, G. M. (2013) Integration of signaling and cytoskeletal remodeling by Nck in directional cell migration. *Bioarchitecture* **3,** 57–63 CrossRef Medline
39. Warner, N., Wybenga-Groot, L. E., and Pawson, T. (2008) Analysis of EphA4 receptor tyrosine kinase substrate specificity using peptide-based arrays. *FEBS J.* **275,** 2561–2573 CrossRef Medline
40. Songyang, Z., Shoelson, S. E., Chaudhuri, M., Gish, G., Pawson, T., Haser, W. G., King, F., Roberts, T., Ratnofsky, S., and Lechleider, R. J. (1993) SH2 domains recognize specific phosphopeptide sequences. *Cell* **72,** 767–778 CrossRef Medline
41. Elowe, S., Holland, S. J., Kulkarni, S., and Pawson, T. (2001) Downregulation of the Ras-mitogen-activated protein kinase pathway by the EphB2 receptor tyrosine kinase is required for ephrin-induced neurite retraction. *Mol. Cell Biol.* **21,** 7429–7441 CrossRef Medline
42. Kriz, V., Agren, N., Lindholm, C. K., Lenell, S., Saldeen, J., Mares, J., and Welsh, M. (2006) The SHB adapter protein is required for normal maturation of mesoderm during *in vitro* differentiation of embryonic stem cells. *J. Biol. Chem.* **281,** 34484–34491 CrossRef Medline
43. Diez-Roux, G., Banfi, S., Sultan, M., Geffers, L., Anand, S., Rozado, D., Magen, A., Canidio, E., Pagani, M., Peluso, I., Lin-Marq, N., Koch, M., Bilio, M., Cantiello, I., Verde, R., *et al.* (2011) A high-resolution anatomical atlas of the transcriptome in the mouse embryo. *PLoS Biol.* **9,** e1000582 CrossRef Medline
44. Bladt, F., Aippersbach, E., Gelkop, S., Strasser, G. A., Nash, P., Tafuri, A., Gertler, F. B., and Pawson, T. (2003) The murine Nck SH2/SH3 adaptors are important for the development of mesoderm-derived embryonic structures and for regulating the cellular actin network. *Mol. Cell Biol.* **23,** 4586–4597 CrossRef Medline
45. Bisson, N., James, D. A., Ivosev, G., Tate, S. A., Bonner, R., Taylor, L., and Pawson, T. (2011) Selected reaction monitoring mass spectrometry reveals the dynamics of signaling through the GRB2 adaptor. *Nat. Biotechnol.* **29,** 653–658 CrossRef Medline
46. Liu, G., Zhang, J., Larsen, B., Stark, C., Breitkreutz, A., Lin, Z. Y., Breitkreutz, B. J., Ding, Y., Colwill, K., Pasculescu, A., Pawson, T., Wrana, J. L., Nesvizhskii, A. I., Raught, B., Tyers, M., *et al.* (2010) ProHits: integrated software for mass spectrometry-based interaction proteomics. *Nat. Biotechnol.* **28,** 1015–1017 CrossRef Medline